Special issue article

SURFACE and INTERFACE ANALYSIS

Received: 26 October 2011 Revised: 30 January 2012 Accepted: 6 February 2012 Published online in Wiley Online Library: 12 April 2012

(wileyonlinelibrary.com) DOI 10.1002/sia.4996

In-situ observation of ion beam-induced nanostructure formation on a $Cu(In,Ga)Se_2$ Surface

Ji Yeong Lee,[a,b] Won Kyung Seong,[b] Minwoong Joe,[b] Kwang-Ryeol Lee,[b] Jong-Ku Park,[b] Myoung-Woon Moon[b]* and Cheol-Woong Yang[a,c]*

We report a phenomenological study of $Cu(In,Ga)Se_2$ (CIGS) dots and their morphological transition into nano-ridge shapes induced by application of a focused ion beam (IB) to CIGS film. Real-time observations of nano-structure evolution during IB irradiation were obtained by recording sequential images at various ion energies of 1 to 30 keV. We observed that as irradiation time increased, the dots became larger and developed elongated ridge structures under continuous sputtering. This transition process was induced by a combination of the Ostwald ripening processes and cluster diffusion. Compositional analysis revealed that the nano-dots changed from pristine CIGS to Cu-rich CIGS. The Ga content of the dots was also found to increase due to sputtered implantation, while levels of In and Se decreased. Copyright © 2012 John Wiley & Sons, Ltd.

Keywords: CIGS; FIB; self-assembly; nanostructure; in-situ SEM

Introduction

Nano-materials have emerged as novel building blocks for the construction of light energy-harvesting assemblies. Size-dependent properties provide the basis for the development of new and effective semiconductor nano-particle systems and for obtaining quantized charging effects in metal nano-particles.[1–3] Nano-structures for use in next-generation energy conversion devices have been designed using innovative strategies.[4,5] Recent efforts to synthesize nano-structures with well-defined geometrical shapes including solid and hollow spheres, prisms, rods, wires, as well as their assembly in two- and three-dimensional structures, have further expanded the possibility of developing novel photovoltaic systems.[6,7]

Current schemes to achieve uniform nano-structural arrays include both top-down and bottom-up approaches. In top-down approaches, nano-structure fabrication is generally accomplished using conventional optical lithography techniques in which feature sizes are limited by the radiation wavelength,[8] while bottom-up methodologies have been utilized primarily in self-assembly techniques such as film growth in strain-induced Stranski - Krastanov mode. These structures can be produced on substrates with different compositions, either amorphous or crystalline, in just a few minutes. In addition, control of the induced nano-structures can be achieved by changing the sputtering parameters, such as ion energy, ion dose, and ion incidence geometry.

Recently, it was reported that $Cu(In,Ga)Se_2$ (CIGS) thin films with nano-structures induced by ion beam (IB) irradiation could be used to modify the band-gap of solar cell systems.[9] In addition, these authors showed that the chemical composition of CIGS nano-structures was altered by the IB irradiation such that the focused IB (FIB)-irradiated CIGS films had a higher content of Cu and a lower content of Se than prior to irradiation.

In this paper, we investigated the mechanism of FIB-induced nano-structure formation on the surface of CIGS thin films. We observed structures comprised of dot and ridge shape nano-structures with dimensions ranging from a few nanometers up to hundreds of nanometers. *In-situ* images of the nano-structures during FIB irradiation were recorded using a scanning electron microscope (SEM). The stoichiometry of these nano-structures was analyzed using a high resolution-transmission electron microscope (TEM) equipped with a scanning TEM (STEM) and energy dispersive X-ray spectrometer (EDS). The effect of IB energy on penetration depth was estimated by Monte Carlo simulation with structural reaction injection modeling (SRIM 2008). The transition mechanism from dot to ridge structures was due to direct coalescence and the Ostwald ripening processes. We suggest that the penetration depth of the incident ions and the sputtering yields of individual elements also play important roles in nano-structure evolution.

Experimental

CIGS thin films were grown by a three-stage process involving the co-evaporation of elemental Cu, In, Ga, and Se on molybdenum-

* *Correspondence to: Prof. C. W. Yang, Affiliation: School of Advanced Materials Science and Engineering, Sungkyunkwan University, Suwon 440–746 Republic of Korea. E-mail: cwyang@skku.edu E-mail: mwmoon@kist.re.kr*

a *Department of Nano Science and Technology, Center for Nanotubes and Nanostructured Composites, Sungkyunkwan University, Suwon, 440-746, Republic of Korea*

b *Future Convergence Research Division, Korea Institute of Science and Technology, Seoul, 130-650, Republic of Korea*

c *School of Advanced Materials Science and Engineering, Sungkyunkwan University, Suwon, 440-746, Republic of Korea*

deposited soda lime glass. The details of the growth process and conditions have been reported previously.[10] Formation of CIGS nano-structures on CIGS surfaces was induced using a commercially available FIB instrument (FEI Nova 600 Nanolab, Ga^+ ion) in a specimen chamber with a base pressure of 5×10^{-6} mbar at room temperature. The incident angle, θ, is defined as the angle of the IB direction to the surface normal; for instance, $\theta = 0°$ means normal incidence to the target surface. Transitions in morphology related to increasing ion doses were observed by *in-situ* SEM monitoring. At fixed ion doses, the size and uniformity of the nano-dots were observed by changing the ion energy of the acceleration voltage. Microstructural and chemical information concerning the IB-induced patterns was obtained using a high-resolution TEM (Tecnai G2 F20, FEI) operating at 200 kV combined with STEM/EDS. The experimental data concerning Ga ion penetration depth into the CIGS layer and sputter yields were compared with those obtained from SRIM calculations.[11]

Results and discussion

Nano-structures were fabricated on CIGS films using Ga^+ IB irradiation, as shown in Fig. 1. We observed a gradual transition in the surface morphology according to increasing IB duration time or ion fluence. CIGS films were exposed to IBs at a normal incidence (or, $\theta = 0°$) and an accelerating voltage of 5 keV. At 1.4×10^{15} ions cm^{-2} (equivalent ion irradiation for 30 s) and 2.8×10^{15} ions cm^{-2} (1 min), nano-dots with an average diameter of 60 nm appeared and grew as shown in Fig. 1(a) and (b). After increasing the ion fluence to 8.6×10^{15} ions cm^{-2} (3 min), round dots were still dominant, but some dots had merged with neighboring dots to form a ridge-like structure. The nano-dots were fully transformed into nano-ridge structures when the ion dose was increased to 1.43×10^{16} ions cm^{-2} (5 min).

We investigated the transition mechanism during Ga^+ IB irradiation by *in-situ* monitoring at an acceleration voltage of 30 keV, an ion current of 0.3 nA, and $\theta = 38°$, as shown in Fig. 2. A plan-view sample of CIGS thin film was prepared for IB irradiation. The whole process can be divided into two stages. In the first stage (Fig. 2(a)–(d)), dots developed and grew in the same position for the duration of the IB irradiation. A coarsening phenomenon was clearly observed (Fig. 2(e)–(h)), where the yellow-dashed brackets (marked by 'A') indicate coarsening and merging of neighbor dots. For example, the dot inside the yellow dashed rectangle (marked by 'B') grew larger and became elongated. Under continuous IB irradiation, dots migrated in the opposite direction to the projected IB direction and coalesced, as shown in Fig. 2(i)–(l). As the film became thin enough, incident ion energy was conveyed to the surface of the CIGS thin film. Dots diffused toward the IB with a slight directional walk. Due to continuous ion erosion, the side of the dot opposite to the IB direction was thinner than the forward side. Dots were able to thermodynamically diffuse in the IB direction because of the shadowing effect. This is shown in Fig. 2(i)–(l) by the rectangle marked 'C' and the circle patterns marked 'D' and 'E'. Dots tended to ride up and turn in the counter-clockwise direction. Smaller dots migrated and merged with larger ones. Dynamic coalescence occurred when clusters diffused and grew together upon IB impact.

Several recent papers have investigated the formation and diffusion of Ga droplets caused by IB irradiation of a GaAs substrate. Wei *et al*. suggested that at the melting point, the dynamic balance of directional mass loss and gain can drive droplets into highly ordered patterns.[12] Rose *et al*. studied the FIB-induced formation and diffusion of Ga dots under continuous sputtering

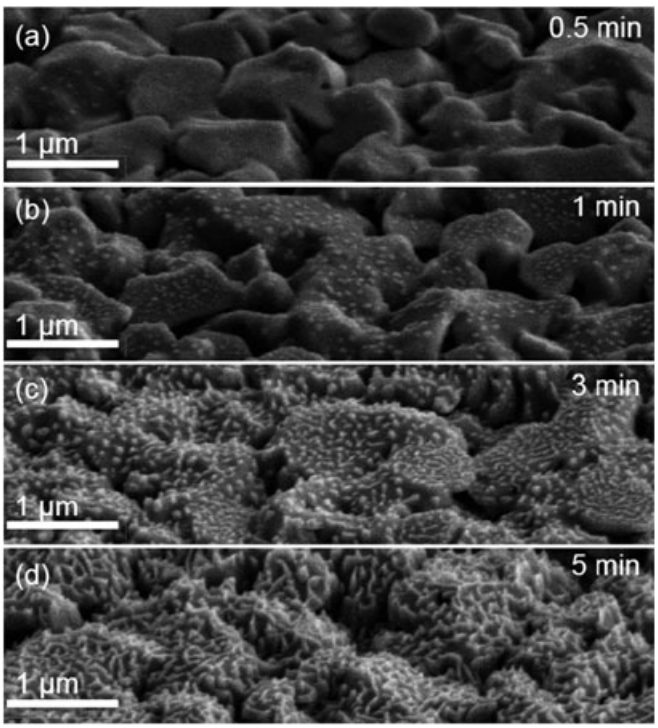

Figure 1. SEM images showing the shape transition in the surface morphology of CIGS films from nano-dots to nano-ridges in response to Ga^+ irradiation at 5 keV and 0.23 nA at a normal incidence for exposure times of (a) 0.5 min (1.43×10^{15} ions cm^{-2}), (b) 1 min (2.8×10^{15} ions cm^{-2}), (c) 3 min (8.6×10^{15} ions cm^{-2}), and (d) 5 min (1.43×10^{16} ions cm^{-2}).

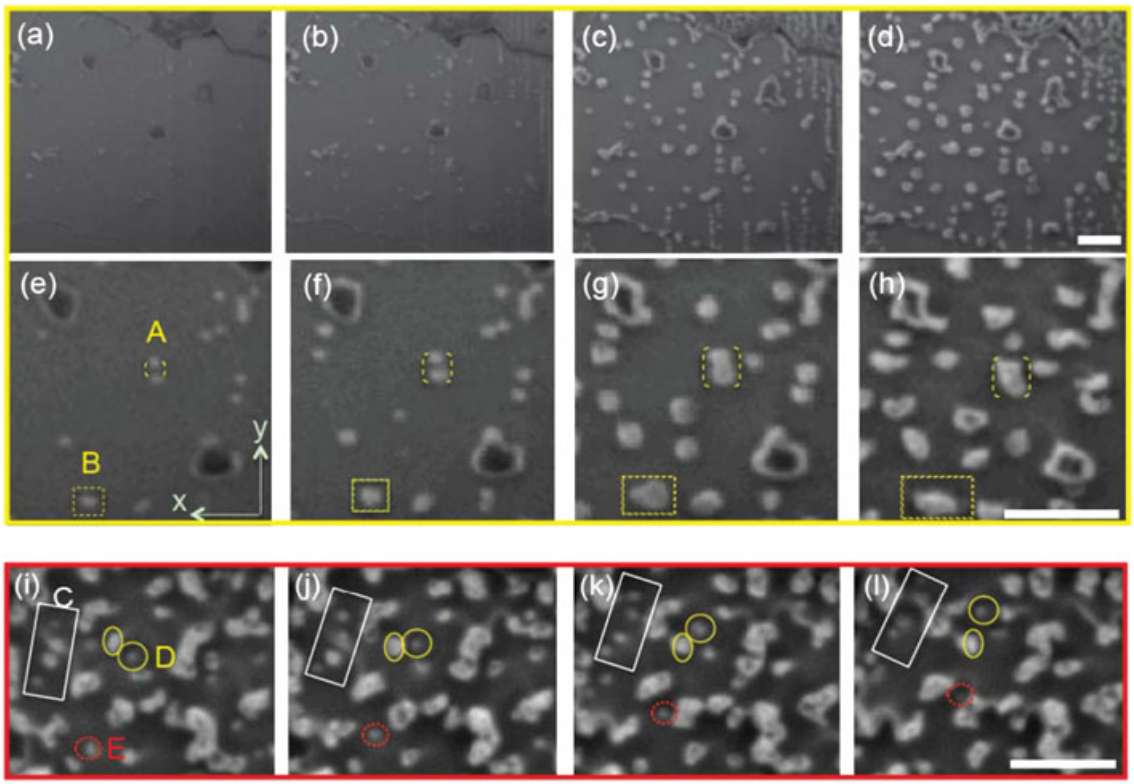

Figure 2. Selected image frames extracted from the FIB movie recorded during Ga^+ irradiation at 30 keV, 0.3 nA, and $\theta = 38^\circ$. (a)–(d) Low magnification series showing the time evolution of nano-structures. The sputtered area of (a)-(d) is $12 \times 10\ \mu m^2$. (e)–(h) magnified series taken from (a)–(d), respectively, showing the coarsening phenomenon in detail. (i)–(l) images show cluster diffusion. The scale bar indicates 500 nm.

on the surface of GaAs substrates. These authors suggested that the diffusion coefficient of Ga dots is 1.68 $\mu m^2\ s^{-1}$and that the dots self-assemble and form ripples.[13] Callegari *et al.* also investigated FIB-induced spontaneous growth of In nano-dots on InP. They suggested that the excess quantity of In induced by different sputter rates tended to aggregate thereby forming nano-dots. The average size of these nano-dots increased with increasing ion fluence and temperature.[14] In this study, we observed dot or nano-ridge formation and cluster diffusion behavior in FIB-irradiated CIGS films. Continuous IB irradiation caused nano-dots to form and adopt a ridge-like structure. This transition mechanism is similar to the clustering phenomenon. The process of clustering can be considered to comprise three stages: nucleation, early stage growth, and late stage growth.[15] During the initial cluster formation, nucleation is an energy barrier to achieve a lower energy state. After this stage, in the early stage growth regime, the cluster grows, capturing atoms from the supersaturated adatom phase. When the adatom concentration reaches its equilibrium value, the cluster distribution can continue to evolve by cluster-cluster processes such as ripening and coalescence; this regime is referred to as late stage growth.

The size of nano-dots is related to the process time by $D \sim t^n$, where D is the diameter of a dot and n is the growth exponent, which depends on the underlying growth mechanism. For example, $n = 0.25$ results in coarsening driven by direct coalescence, while $n = 0.33 - 0.5$ results in Ostwald ripening.[16–18] The Ostwald ripening mechanism refers to the growth of large dots at the expense of small dots. We observed that a single dot (see Fig. 2 (e)–(h)) coarsened in a power-law fashion with $n = 0.42$ as the duration of radiation exposure increased (Fig. 3), indicating Ostwald ripening. Thus, the IB irradiation-induced coarsening of CIGS dots was governed mainly by Ostwald ripening. During the early stage, direct coalescence of adjacent dots due to coarsening of individual dots was observed. However, at the late growth stage, cluster diffusion also occurred. Overall, the coarsening of CIGS dots shown in Fig. 2 occurred due to the combination of Ostwald ripening and cluster diffusion.

A SEM image of the surface morphology of CIGS film after Ga^+ ion irradiation at 30 keV with 5.7×10^{14} ions cm^{-2} at a normal incidence is presented in Figure 4(a). Nano-dots with a diameter of 50 nm formed on the surface of the CIGS film. We performed

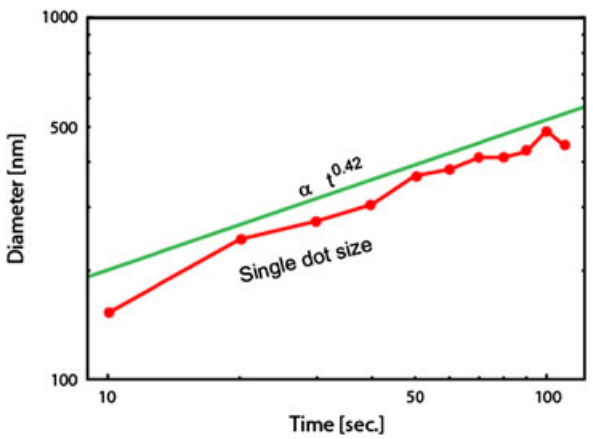

Figure 3. Diameter-measured curve of a single dot during ion beam irradiation. The diameter of the dot was measured at 10 s intervals from the recorded movie described in Fig. 2. Growth of the nano-dot follows a power law with a growth exponent of $n = 0.42$, indicative of Ostwald ripening. The straight line represents the least squares fit.

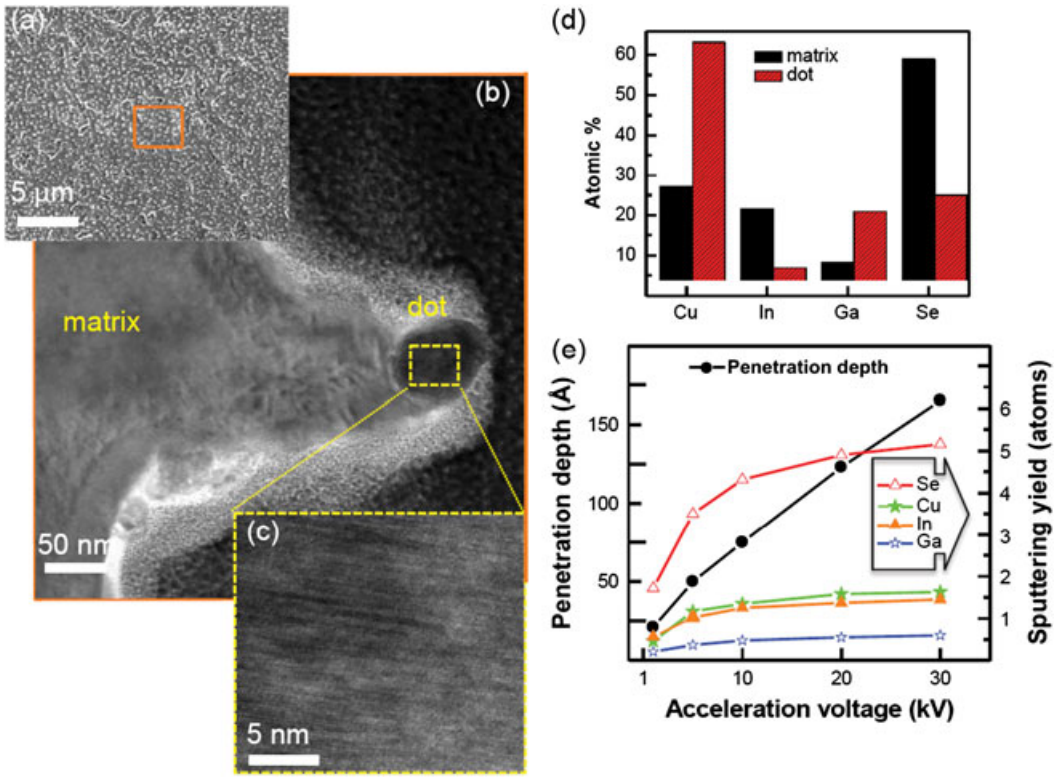

Figure 4. (a) CIGS surface after Ga^+ irradiation at 30 keV with 5.7×10^{14} ions cm^{-2} at normal incidence. (b) Cross-sectional TEM image of a dot formed on the CIGS film and (c) its HR-TEM image. (d) The elemental composition graph inside the CIGS film (matrix) and the dot region (dot), as marked in (b). (e) SRIM 2008 simulation results showing that the penetration depth of incident ions and the sputtering yields of elements on the CIGS film as a function of accelerating voltage.

cross-sectional analysis as shown in Fig. 4(b) using transmission electron microscopy. A lattice fringe of dots was clearly visible (see Fig. 4(c)). The elemental composition of dots was significantly altered by Ga^+ ion irradiation, as shown in Fig. 4(d). We estimated that the Se content halved, while the Cu content doubled. The increase in the fraction of Cu is the result of the faster diffusivity of Cu compared to the other components.[9] Different sputter yields would also induce this compositional change on the CIGS surface. The Ga content increased considerably; it was about four times higher than before IB irradiation due to the low sputtering yield and Ga ion implantation. Sputter yields of individual elements in the CIGS film were calculated using SRIM calculations, as shown in Fig. 4(e). An incidence angle of Ga of 0° (normal to the target surface) and 500 ions were used in the calculations. The preferential sputtering yield was Se (5.16) > Cu (1.63) > In (1.45) > Ga (0.60) at 30 keV. The energies of Ga ions varied from 1 to 30 keV. The driving force of compositional change was clustering of the remaining elements on the surface. The penetration depth of incident Ga ions was recorded by estimating the number of particles at a given depth from the surface by Gaussian fitting. As acceleration voltage increased, the penetration depth increased both laterally and longitudinally. The penetration depth had a large impact on the size of the ion-induced dots; deeply penetrated ions introduce defects into film.

The energy dependency of dot configuration is shown in Fig. 5. In the case of 1 keV in Fig. 5(a), very small dots were obtained at an ion fluence of 1×10^{15} ions cm^{-2}, while round dots transitioned into nano-ridge structures as the ion fluence increased to 2×10^{16} ions cm^{-2} in Fig. 5(b). As the ion energy increased, the size of the dots increased, but no ridge structures formed at a fixed ion fluence of 2×10^{16} ions cm^{-2} (Fig. 5(c) and (d)). The average diameters of dots were estimated to be 16.0 ± 6.29, 19.5 ± 4.6 and 46.2 ± 15.2 for energies of 1, 5, and 30 keV, respectively. At lower acceleration voltages, nano-dots were uniformly distributed and had a higher density than dots distributed at the higher acceleration voltage of 30 keV.

Conclusions

We observed self-assembled CIGS nano-structure formation and transition from dot to nano-ridge structures under Ga^+ IB irradiation at various energy levels from 1 to 30 keV by *in-situ* observation. As the ion fluence increased, the nano-dots ripened, and some dots became elongated. The transition from dots to ridge-like structures was explained by the Ostwald ripening process and cluster diffusion. In addition, we suggested that the sputtering yield of individual elements and the penetration depth of incident ions affected nano-structure development. Based on TEM observations, we confirmed that ion-induced dots maintained a high degree of crystallinity despite their markedly altered chemical composition. The Cu content of the IB-induced nano-dots was higher than that of the pristine CIGS film, while the content of Se was significantly reduced. The Ga content in the IB-treated CIGS films was much higher than that of the pristine CIGS films due to the low diffusivity of Ga ions as well as Ga^+ ion implantation. The size and distribution of nano-dots were also influenced by the accelerating ion energy.

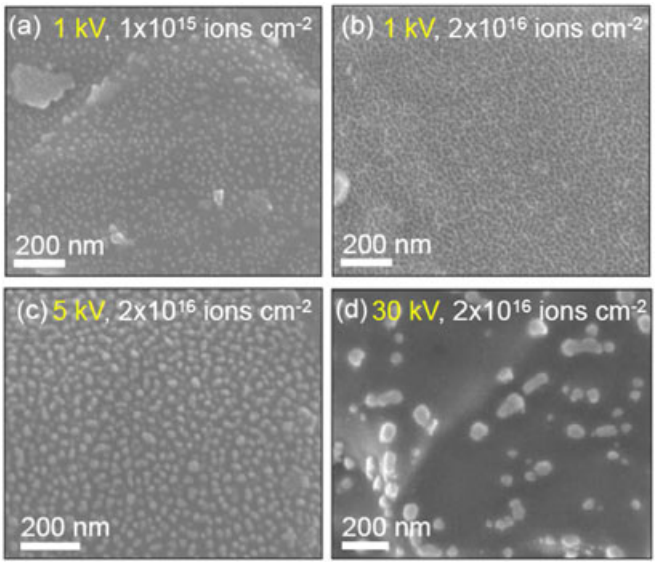

Figure 5. SEM images showing dot evolution at normal beam incidence for ion energies of (a) 1 keV (at an ion fluence of 1×10^{15} ions cm^{-2}), (b) 1 keV (2×10^{16} ions cm^{-2}), (c) 5 keV (2×10^{16} ions cm^{-2}), and (d) 30 keV (2×10^{16} ions cm^{-2}).

Acknowledgements

This research was supported in part by grant from the R&D program under the Korea Ministry of Knowledge Economy, the internal project of KIST, and by the National Research Foundation of Korea grant funded by the Korea government (MEST) (No. 2011–0019984). The authors gratefully appreciate support from CCRF and CNNC at Sungkyunkwan University.

References

[1] M. L. Steigerwald, L. E. Brus, *Acc. Chem. Res.* **1990**, *23*, 183.
[2] H. Weller, *Adv. Mater.* **1993**, *5*, 88.
[3] L. Banyai, S. W. Koch, World Scientific Publishing Co., River Edge, NJ, **1993**.
[4] P. V. Kamat, *J. Phys. Chem. B* **2002**, *106*, 7729.
[5] K. George Thomas, P. V. Kamat, *Acc. Chem. Res.* **2003**, *36*, 888.
[6] Y. N. Xia, P. D. Yang, Y. G. Sun, Y. Y. Wu, B. Mayers, B. Gates, Y. D. Yin, F. Kim, Y. Q. Yan, *Adv. Mater.* **2003**, *15*, 353.
[7] M.D. Regulacio, M. Y. Han, *Acc. Chem. Res.* **2010**, *43*, 621.
[8] T. Ito, S. Okazaki *Nature* **2000**, *406*, 1027.
[9] J. Y. Lee, Sk. F. Ahmed, M.-H. Park, S.-K. Ha, J.-K. Park, K.-R. Lee, W. J. Choi, J. H. Yun, S. J. Ahn, M.-W. Moon, C.-W. Yang, submitted to *Sol. Energy Mater. Sol. Cells*, **2011**.
[10] K. H. Kim, K. H. Yoon, J. H. Yun, B. T. Ahn, *Electrochem. Solid-State Lett.* **2006**, *9*, A382.
[11] J. F. Ziegler, SRIM-The Stopping and Range of Ions in Matter, http://www.srim.org, **2012**.
[12] W. Wei, J. Lian, W. Lu, and L. Wang, *Phys. Rev. Lett.* **2008**, *100*, 076103.
[13] F. Rose, H. Fujita, H. Kawakatsu, *Nanotehnology* **2008**, *19*, 035301.
[14] V. Callegari, P. M. Nellen, *Phys. Stat. Sol.* (a) **2006**, *204*, 1665.
[15] M. Z. Allmang, L. C. Feldman, M. H. Grabow, *Surf. Sci. Rep.* **1992**, *16*, 377.
[16] J. H. Yao, K. R. Elder, H. Guo, M. Grant, *Phys. Rev. B* **1993**, *47*, 14110.
[17] J.-W. Hong, J.-H. Pyeon, J. Tedesco, Y.-B. Park, *Phys. Rev. B* **2007**, *75*, 1.
[18] M. Stepanova, S. K. Dew, *J. Phys. Condensed. Matter* **2009**, *21*, 224014.